



# Systematic design of active constraint switching using selectors<sup>☆</sup>

Dinesh Krishnamoorthy\*, Sigurd Skogestad

Department of Chemical Engineering, Norwegian University of Science and Technology (NTNU), Trondheim, Norway



## ARTICLE INFO

### Article history:

Received 11 July 2020

Revised 29 August 2020

Accepted 22 September 2020

Available online 24 September 2020

## ABSTRACT

Selector logic is a simple and effective tool to switch between different controlled variables associated with change in active constraints. Selector blocks have been extensively used in the process control industry for decades, but their design has been based on engineering intuition and experience. Currently, there is a lack of systematic procedure to design selectors for active constraint switching. In this paper, we address this gap and provide a systematic procedure, which can be applied without the need for detailed process models. Illustrative examples are used to demonstrate the proposed framework.

© 2020 The Authors. Published by Elsevier Ltd.

This is an open access article under the CC BY license (<http://creativecommons.org/licenses/by/4.0/>)

## 1. Introduction

Selector logic blocks, also commonly known as *overrides* have been in use in the process industries for several decades to switch between a plurality of controllers, and are available as a part of any standard digital control system (DCS) software package. Despite their widespread use, not just in the process industries, but also in other application domains, selectors are currently designed in an ad-hoc fashion based on engineering know-how and experience (Liptak, 2003, Section 1.17).

There is a lack of systematic design procedure that tells when to use a max-selector, when to use a min-selector, and when is it not feasible to use a selector. Industry-oriented and process control books such as (Shinskey, 1996, Ch. 6), (Wade, 2004, Ch. 12), (Seborg et al., 2010, Ch. 18), (Smith and Corripio, 2006, Ch. 10) and (Marlin, 2000, Ch. 22) demonstrate the use of selectors using various illustrative examples, but there is no systematic procedure. Glattfelder and Schaufelberger (2012) studies several control structures, however the analysis is limited to only one CV constraint, and does not address the case with several CV constraints. Although there have been a few works studying the stability of min-max selectors, see for example (Foss, 1981), (Imani and Montazeri-Gh, 2020), (Glattfelder and Schaufelberger, 1983) and the references therein, the choices that affect design of the selectors itself still remains an open problem.

<sup>☆</sup> The authors gratefully acknowledge the financial support from SUBPRO, which is financed by the Research Council of Norway, major industry partners and NTNU.

\* Corresponding author:

E-mail addresses: [dinesh.krishnamoorthy@ntnu.no](mailto:dinesh.krishnamoorthy@ntnu.no) (D. Krishnamoorthy), [skoge@ntnu.no](mailto:skoge@ntnu.no) (S. Skogestad).

In this paper, we address this gap by providing a systematic design procedure. In particular, we study the use of selectors for active constraint switching in the context of economic optimal operation.

Often optimal operation occurs when some of the constraints are at their limiting values. For example, when the market price for the product is high, then the process should be operated at its maximum production capacity, in order to maximize the profit. Constraints that are optimally at their limiting values are known as *active constraints*. Because of changes in the operating conditions (disturbances) and market prices, the set of active constraints changes. An *active constraint region* is a disturbance space that is defined by the set of constraints that are active within it (Jacobsen and Skogestad, 2011).

Typically, real-time optimization (RTO) involves solving a numerical optimization problem using rigorous nonlinear process models to compute the optimal setpoints, which are given to the control layer below. Recently, there is an increasing interest in achieving optimal operation, without the need to solve numerical optimization problems (Srinivasan and Bonvin, 2019), (Chachuat et al., 2009), (Engell, 2007), (Krishnamoorthy and Skogestad, 2020, 2019), (Reyes-Lúa and Skogestad, 2020), (Jagtup et al., 2013). In other words, the economic objectives are translated into control objectives, thereby achieving optimal operation using simple feedback control structures (Skogestad, 2000). The idea of "feedback optimizing control" dates back to Morari et al. (1980). The main idea of feedback optimizing control (also sometimes referred to as self-optimizing control Skogestad (2000), or direct input adaptation (Chachuat et al., 2009)) is to find the right set of controlled variables (CVs), which when held constant, leads to economically optimal operation (Morari et al., 1980), (Skogestad, 2000).

When some of the constraints are optimally active, then the simplest approach is to control the constraints at their limits, possibly with some safety margin, known as *back-off*. This is known as *active constraint control*. If there are any remaining unconstrained degrees of freedom (manipulated variables), one should then identify *self-optimizing* controlled variables, for example the steady-state cost gradient. Note that, Skogestad (2000) included the active constraints as the "obvious" self-optimizing variables, and the theory of self-optimizing control was developed for the less obvious unconstrained CVs (Jäschke et al., 2017).

Mathematically, feedback optimizing control aims to find a simple feedback solution to a steady-state real-time optimization problem of the form

$$\min_{\mathbf{u}} J(\mathbf{x}, \mathbf{u}, \mathbf{d}) \tag{1a}$$

s.t.

$$\mathbf{g}(\mathbf{x}, \mathbf{u}, \mathbf{d}) \leq 0 \tag{1b}$$

where  $\mathbf{u} \in \mathbb{R}^{n_u}$  are the set of manipulated variables (MV),  $\mathbf{x} \in \mathbb{R}^{n_x}$  denotes the internal variables,  $\mathbf{d} \in \mathbb{R}^{n_d}$  denotes the set of disturbances,  $J : \mathbb{R}^{n_u} \times \mathbb{R}^{n_x} \times \mathbb{R}^{n_d} \rightarrow \mathbb{R}$  is the cost function, and  $\mathbf{g} : \mathbb{R}^{n_u} \times \mathbb{R}^{n_x} \times \mathbb{R}^{n_d} \rightarrow \mathbb{R}^{n_g}$  are the set of constraints. A constraint  $g_i(\mathbf{x}, \mathbf{u}, \mathbf{d}) \leq 0$  is said to be active if  $g_i(\mathbf{x}, \mathbf{u}, \mathbf{d}) = 0$ . Let the set of  $n_a \leq n_g$  active constraints be denoted by  $\mathbf{g}_A \subseteq \mathbf{g}$  (i.e.  $\mathbf{g}_A(\mathbf{x}, \mathbf{u}, \mathbf{d}) = 0$ ).

Note that here, the manipulated variables  $\mathbf{u}$  denote the available degrees of freedom for the given problem. It may either be the actual physical manipulated variable, or the setpoint to a lower level regulatory controller.

To transform the optimization problem into a feedback control problem, we need to identify controlled variables (CVs  $y_i$ ) associated with the constraints and the with the goal of minimizing the cost  $J$ . The latter is a bit complicated, as the best "self-optimizing" variables to control for minimizing the cost  $J$  depends on what the active constraints are. Thus, for a steady-state optimization problem of the form (1), the first step towards designing a feedback optimizing control structure involves identifying the relevant active constraint combinations. Once the relevant active constraint combinations are identified, one must make a decision on which unconstrained variables to control. That is, in each active constraint region, we must control (Krishnamoorthy and Skogestad, 2020),

1. The  $n_a$  active constraints at their limits (i.e. CV:=  $\mathbf{g}_A \rightarrow 0$ ),
2. For the remaining  $n_u - n_a$  unconstrained degrees of freedom, control a self-optimizing controlled variable (unconstrained CV), e.g. the steady-state cost gradient.

It is then evident, that the active constraint regions play an important role in feedback optimizing control, since this determines "what to control". However, most of the works considering feedback optimizing control (studied in the context of extremum seeking control (Ariyur and Krstic, 2003), NCO-tracking (François et al., 2005), self-optimizing control (Skogestad, 2000), hill-climbing control (Kumar and Kaistha, 2014), neighboring extremal control (Gros et al., 2009) etc. to name a few) focus on the unconstrained optimum, and switching between active constraint sets has received relatively little attention. One of the main reasons for this is probably that active constraint control is often seen as simple/obvious.

When the set of active constraints changes, then this requires a change in the controlled variables and reconfiguration of the control loops. The active constraints may be on the controlled variables (CV), or on the manipulated variables (MV). Therefore, optimal operation may involve either CV-CV switching, MV-MV switching, or CV-MV switching.

CV-CV switching occurs when there are several CV constraints for one MV, but only one CV constraint is active and can be con-

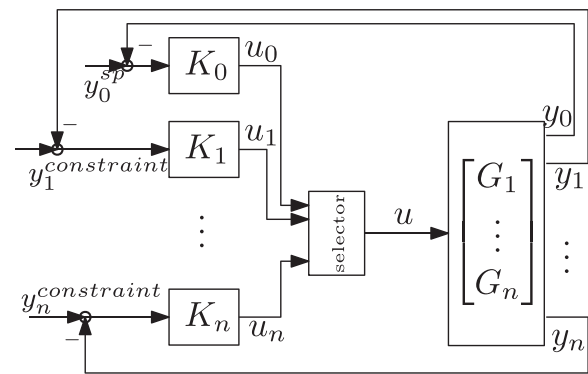


Fig. 1. Schematic representation of active constraint switching using selectors.

trolled at any given time. To achieve this using selectors, independent controllers may be designed for each controlled variable, and a max/min-selector is used to select either the maximum or the minimum value of all the inputs computed by the different controllers as shown in Fig. 1 for the case where all the constraints are associated with a single input  $u$ . This is the case studied in this paper.

The main contribution of this paper is the systematic design procedure for active constraint switching using selectors for the case when all the constraints are associated with a single input. Several illustrative examples are provided to demonstrate the proposed systematic design procedure.

## 2. Motivating example 1: Gas turbine control

Consider a gas turbine engine in Fig. 2 (e.g. for power generation or for aircraft propulsion) with two MVs (degrees of freedom), namely the air inflow rate  $F_a$  and the fuel injection rate  $u$ . Suppose the objective is to control the engine power  $y_0 = W$  to a desired setpoint, subject to a max-constraint on the rotational speed  $\omega$ , a max-constraint on the engine temperature  $T_e$ , a min-constraint on the engine pressure  $p_e$ , a min-constraint on the air inlet pressure  $p_a$ , and a max-constraint on the fuel injection rate  $u$  (MV),

$$\text{Desired: } y_0 = W = W_{sp}$$

$$\text{CV constraints: } y_1 = \omega \leq \omega_{max}$$

$$y_2 = T_e \leq T_{e,max}$$

$$y_3 = p_e \geq p_{e,min}$$

$$y_4 = p_a \geq p_{a,min}$$

$$\text{MV constraint: } u \leq u_{max}$$

Assuming that the air inflow rate  $F_a$  is used to control the engine temperature  $T_e$  to its maximum value  $T_{e,max}$ , the fuel injection rate must be used to achieve the other objectives. In the reduced system, we have one CV ( $y_0 = W$ ) with a desired setpoint which may

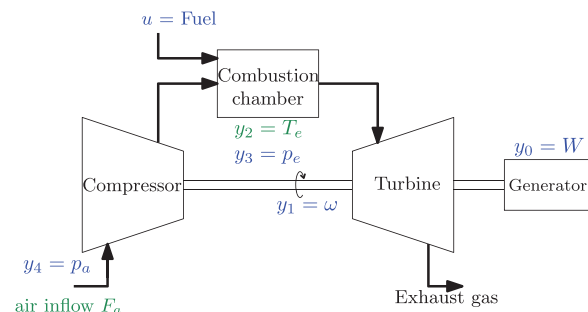


Fig. 2. Schematic representation of a gas turbine engine.

be given up if necessary, three CVs  $y_i$ ,  $i = \{1, 3, 4\}$  with inequality constraints, and one MV  $u$  with an upper limit.

Process insight tells us that increasing the fuel  $u$  will increase the speed  $y_1 = \omega$ , increase the engine pressure  $y_3 = p_e$ , and decrease the air inlet pressure  $y_4 = p_a$ . Based on this, if one uses a min-selector to switch between the CVs, the constraints on  $u$ ,  $y_1$ , and  $y_4$  would remain feasible, but the minimum constraint on  $y_3$  may be violated. Similarly, with a max-selector,  $y_3$  would remain feasible, but constraints on  $u$ ,  $y_1$ , and  $y_4$  may be violated. It is also not evident if the performance would be the same if one were to use a max-min selector or a min-max selector in series, if so under what conditions.

This simple example clearly shows that although one can often design selector blocks using process insight in such an ad-hoc fashion, it is clearly desirable to have a more systematic procedure in order to design verifiable control structures. Specifically, it may not be evident to an engineer when a set of constraints are conflicting, whether to use a min or a max-selector, or a combination of both, or if such a switching scheme is feasible at all. Also, the lack of a systematic design procedure means that all the feasible alternatives may not be explored.

### 3. Systematic design of active constraint switching using selectors

Consider a process with a single input ( $u$ ) and many potential controlled variables (CVs), such that we have

- At most one CV ( $y_0$ ) with a desired setpoint, that may be given up if necessary.
- Any number of CV  $y_i$  with inequality constraints  $y_{i,lim}$ , that may be optimally active.
- MV inequality constraints  $u_{min} \leq u \leq u_{max}$

Note that the objective is to achieve feasible and optimal steady-state operation using simple feedback controllers and selectors to switch between the active constraints. Therefore, the following results are based on steady-state.

Notation:

- Let  $G_i$  denote the steady state gain from the input  $u$  to the output  $y_i$ .
- Let  $\mathbb{Y}$  be the set of all inequality constraints  $y_{i,lim}$  (where  $y_{i,lim}$  could be both  $y_{i,max}$  or  $y_{i,min}$ ) that needs to be satisfied at steady-state for any given operating condition.

**Assumption 1.** The gain  $G_i$  from  $u$  to  $y_i$  does not change sign (that is,  $\frac{dy_i}{du}$  has the same sign for any  $du$  and any operating point).

The set of constraints can be divided into two subsets  $\mathbb{Y} = \mathbb{Y}^+ \cup \mathbb{Y}^-$  according to the following criteria.

1.  $\mathbb{Y}^+$  is the set of constraints where reducing the input  $u$  is better in terms of satisfying the constraints. This means that
  - For CVs where the gain  $G_i$  from  $u$  to  $y_i$  is positive ( $G_i > 0$ ), the set  $\mathbb{Y}^+$  includes the corresponding max-constraints ( $y_{i,max}$ ).
  - For CVs where the gain  $G_i$  from  $u$  to  $y_i$  is negative ( $G_i < 0$ ), the set  $\mathbb{Y}^+$  includes the corresponding min-constraints ( $y_{i,min}$ ).
  - The set  $\mathbb{Y}^+$  also includes a possible max-constraint on  $u$  ( $u_{max}$ ).
2.  $\mathbb{Y}^-$  is the set of constraints where increasing the input  $u$  is better in terms of satisfying the constraints. This means that
  - For CVs where the gain  $G_i$  from  $u$  to  $y_i$  is positive ( $G_i > 0$ ), the set  $\mathbb{Y}^-$  includes the corresponding min-constraints ( $y_{i,min}$ ).

- For CVs where the gain  $G_i$  from  $u$  to  $y_i$  is negative ( $G_i < 0$ ), the set  $\mathbb{Y}^-$  includes the corresponding max-constraints ( $y_{i,max}$ ).
- The set  $\mathbb{Y}^-$  also includes a possible min-constraint on  $u$  ( $u_{min}$ ).

Define

$$u_i = u(y_i = y_{i,lim}) \tag{2}$$

as the value of the input  $u$  which at steady-state satisfies the constraint  $y_{i,lim}$ , i.e.,  $u_i$  gives  $y_i = y_{i,lim}$  at steady state.

**Theorem 1 (Feasibility).** Let

$$\bar{u} = \min_{i \in \mathbb{Y}^+} u_i \tag{3}$$

denote the largest allowed input  $u$  that satisfies all the constraint in the set  $\mathbb{Y}^+$ , and similarly, let

$$\underline{u} = \max_{i \in \mathbb{Y}^-} u_i \tag{4}$$

denote the smallest allowed input  $u$  that satisfies all the constraint in the set  $\mathbb{Y}^-$ . Then to have feasible operation using  $u$  as the manipulated variable, we must at any given steady-state operating point have  $\underline{u} \leq u \leq \bar{u}$ .

**Proof.** To remain feasible, we need  $u \leq \bar{u}$  to satisfy the constraints in  $\mathbb{Y}^+$  and  $u \geq \underline{u}$  to satisfy the constraints in  $\mathbb{Y}^-$ . Satisfying both these conditions is possible if and only if  $\underline{u} \leq \bar{u}$ .  $\square$

**Theorem 1** tells when satisfying all constraints is feasible using a single input  $u$ , that is, when there is an allowable operating window for  $u \in [\underline{u}, \bar{u}]$ . If we have infeasibility (conflicting constraints) according to **Theorem 1**, then we have two possibilities:

1. let another input (MV)  $v$  take over the control of one of the constraints which is no longer controlled using  $u$ . This will involve MV-MV switching from input  $u$  to  $v$  (see discussions in [Section 6.5](#)).
2. If we dont have another MV  $v$  to take control of the conflicting constraints, then one would have to prioritize the constraints and give up the less important constraint (this will be formally stated later in [Theorem 3](#)).

**Theorem 1** only tells us when the constraints are feasible. To get a unique value for  $u$  we need to add another objective. Typically, we have a controlled variable ( $y_0$ ) with a desired setpoint, and if possible we want to use the corresponding value of input ( $u_0$ ) which gives  $y = y_0$  at steady-state. More generally, the desired input may result from an optimization problem,

$$u^* = \arg \min_u \{J(u, d) \mid \text{s.t. CV and MV constraints}\} \tag{5}$$

with  $u^*$  being the unique minimizer of (5). Then  $u_0$  is the value of  $u^*$  for the corresponding unconstrained problem;

$$u_0 = \arg \min_u J(u, d) \tag{6}$$

We may also have cases where the objective is to maximize or minimize some variable. This will correspond to having  $u_0 = \infty$  or  $u_0 = -\infty$  (for the corresponding unconstrained problem).

**Theorem 2 (Optimality).** Assume the operational objective is to minimize  $J$ , and let  $u_0$  denote the value of the input  $u$  that minimizes  $J$  for the unconstrained case. Assuming feasible operation, so that  $\underline{u} < \bar{u}$  ([Theorem 1](#)), the optimal input  $u$  is given by

$$u^* = \text{mid}(\bar{u}, u_0, \underline{u}) \tag{7}$$

**Proof.** If  $\underline{u} < u_0 < \bar{u}$  then the unconstrained optimum is within the feasible region, and optimal operation occurs when  $u^* = u_0$ . This is schematically represented in [Fig. 3a](#).

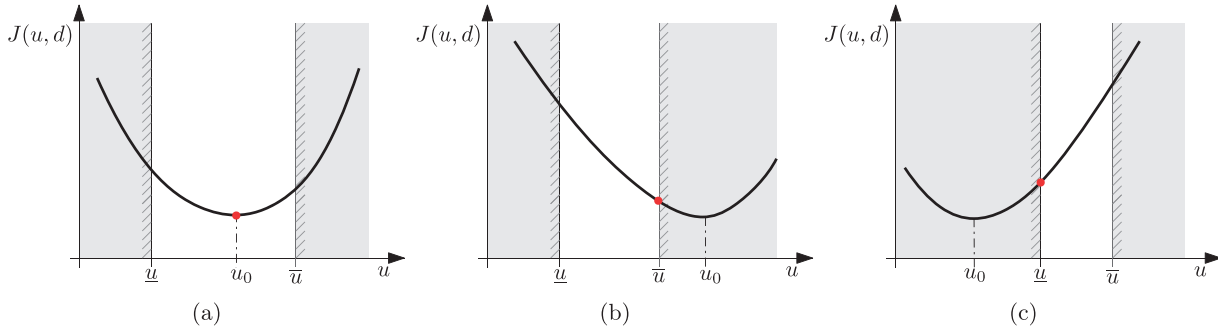


**Fig. 3.** Schematic representation showing that the optimal input (marked with a red dot) can be achieved using a mid-selector. (a) Unconstrained Optimum  $\bar{u} < u_0 < \underline{u}$ . (b) Constrained optimum  $\underline{u} < \bar{u} < u_0$ . (c) Constrained optimum  $u_0 < \underline{u} < \bar{u}$ .

If  $\underline{u} < \bar{u} < u_0$ , then  $u_0$  is infeasible. Hence  $u^* = \underline{u}$  (see Fig. 3b). Similarly, if  $u_0 < \underline{u} < \bar{u}$ , then  $u_0$  is infeasible. Hence  $u^* = \bar{u}$  (see Fig. 3c). □

For implementation, we assume that we have several SISO controllers that compute the desired input  $u_i$  for each CV  $y_i \in \mathbb{Y}$ . If these controllers have integral action, then we must design a suitable anti-windup scheme (Åström, 1987), which is discussed later in Section 6.4.

There are several ways the result in Theorem 2 can be implemented using selectors. The most obvious is with three selector blocks; a max- and min-selector for  $\underline{u}$  and  $\bar{u}$ , respectively, and a mid-selector for  $u$  as shown with the max/min-mid structure in Fig. 4a.

$$u = \text{mid}(\bar{u}, u_0, \underline{u}) \tag{8}$$

However implementations with only two selectors are also generally possible. This is further discussed in the following remark.

**Remark 1** (Two selector blocks). If we have feasibility, the mid-selector (8) is equivalent to using a combined minimum and maximum selector block in series which may be in any order.

Min-Max structure (Fig. 4b)

$$u = \max_{j \in \mathbb{Y}^-} \{u_j\}, \underbrace{\min(u_0, \{u_i\})}_{=\bar{u}'} \tag{9}$$

Max-Min structure (Fig. 4c)

$$u = \min_{i \in \mathbb{Y}^+} \{u_i\}, \underbrace{\max(u_0, \{u_j\})}_{=\underline{u}'} \tag{10}$$

Note that here, the last selector block will always be satisfied. In the min-max structure, the constraints  $\mathbb{Y}^+$  are masked and  $\mathbb{Y}^-$  will always be satisfied. Similarly, in the max-min structure, the constraints  $\mathbb{Y}^-$  are masked and  $\mathbb{Y}^+$  will always be satisfied (Glattfelder and Schaufelberger, 2012). Table 1 shows a numerical example to illustrate that the three structures studied in Fig. 4 are

**Table 1**

Numerical example illustrating that the three structures in Fig. 4 are equivalent when the set of constraints are feasible (Cases 1–3), but when  $\bar{u} < \underline{u}$  (infeasibility), they differ (cases 4–6).

cases	$\underline{u}$	$\bar{u}$	$u_0$	mid (Fig. 4a)	min-max (Fig. 4b)	max-min (Fig. 4c)
1	1	10	5	5	5	5
2	1	10	12	10	10	10
3	1	10	0	1	1	1
4	10	1	5	5	10	1
5	10	1	12	10	10	1
6	10	1	0	1	10	1

equivalent when the set of constraints are feasible (cases 1, 2 and 3). It also shows the difference in the different structures in terms of responding to infeasibility (cases 4, 5 and 6 when  $\bar{u} < \underline{u}$ ), which is formalized in the theorem below.

**Theorem 3** (Selector design for conflicting constraints). *If the constraints are conflicting, that is,  $\bar{u} < \underline{u}$  and Theorem 1 does not hold, then*

- the min-max structure in Fig. 4b always gives up  $\bar{u}$  corresponding to the constraints in  $\mathbb{Y}^+$
- the max-min structure in Fig. 4c always gives up  $\underline{u}$  corresponding to the constraints in  $\mathbb{Y}^-$
- the mid-selector structure in Fig. 4a gives up  $\bar{u}$ ,  $\underline{u}$ , or both of them, depending on the value of  $u_0$ .

**Proof.** The result follows quite trivially by considering what happens if we don't have feasibility, that is, when  $\bar{u} < \underline{u}$ . Since any downstream selector masks all previous selections, a min-max selector always chooses  $u = \underline{u}$ , and a max-min selector always chooses  $u = \bar{u}$ . This is also illustrated for a numerical example in Table 1, and by replacing the entries in Table 1 with symbols, we would get a general proof. □

Often, the different constraints have different levels of priority, and a common approach to handle infeasibility is to "give-up" the less important constraints. As seen above, the order of the selector blocks plays an important role in deciding which constraints are given up. Consequently, Theorem 3 can be used to decide which structure to use based on the constraint priority level.

In short, Theorem 3 tells us that for the max-min and min-max structures, the constraint entering the last selector block will be prioritized in case of conflicting constraints. That is, the input  $u$  will in cases of conflict "give up" controlling a masked constraint  $y$  with "low priority". However, this does not necessarily mean that we need to give up controlling  $y$ , because it may be possible to let another input (MV)  $v$  take over the task of controlling the masked constraint  $y$ . This will involve MV-MV switching from input  $u$  to  $v$  as discussed in Section 6.5.

One advantage of using the mid-selector in Fig. 4a is that we have explicit calculation of both  $\bar{u}$  (the largest allowed input) and  $\underline{u}$  (the smallest allowed input). This is useful, since it can be used to verify feasibility by checking whether  $\bar{u} > \underline{u}$ . If this is not satisfied, then we may use the value of  $u_0$  to tell which constraint to give up, or even to give up both constraints in a desired manner by selecting an appropriate value for  $u_0$  (see Table 1). The latter, that is, giving up both of the conflicting constraints, is not possible with the max-min or min-max structures.

There are also special cases where only a single selector block is sufficient.



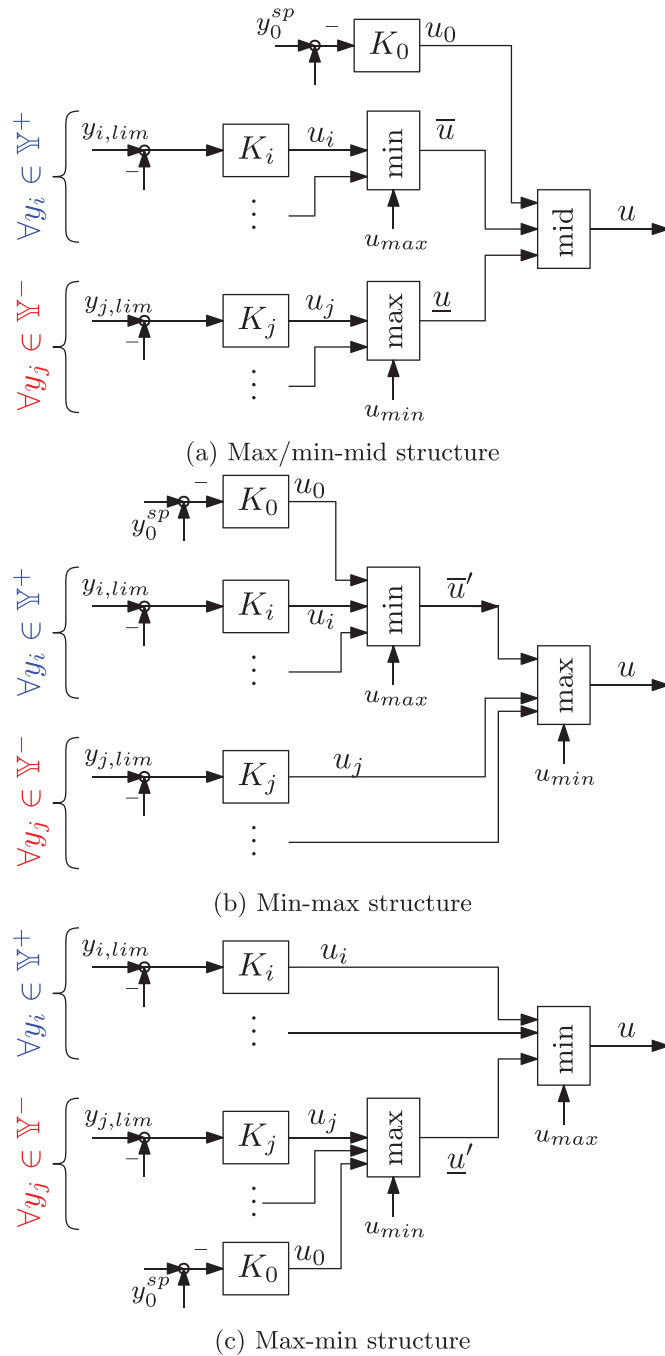


**Fig. 4.** CV-CV and CV-MV switching using selectors. The three alternative structure (a), (b) and (c) are equivalent if we have feasibility, that is, [Theorem 1](#) holds.

**Remark 2** (Single selector block). If  $\mathbb{Y}^- = \emptyset$  (i.e. we only have constraints where reducing the input  $u$  is better in terms of satisfying the constraints), then the solution is always feasible and the optimal input  $u$  is given using a minimum selector

$$u^* = \min(u_0, \bar{u}) \quad (11)$$

This is a special case of [Fig. 4b](#) without the max-selector.

Similarly, if  $\mathbb{Y}^+ = \emptyset$  (i.e. we only have constraints where increasing the input  $u$  is better in terms of satisfying the constraints), then the solution is always feasible and the optimal input  $u$  is given using a max-selector

$$u^* = \max(u_0, \underline{u}) \quad (12)$$

This is a special case of [Fig. 4c](#) without the min-selector.

Finally, if there is one constraint in the set  $\mathbb{Y}^+$  and one constraint in the set  $\mathbb{Y}^-$ , we can use a single mid-selector. This is a special case of [Fig. 4a](#) without the min- and max-selectors

The systematic design procedure of the selectors for the case with a single MV ( $u$ ) can be summarized by the following steps:

- Step 1. Group the list of constraints into two sets, namely the set  $\mathbb{Y}^+$  and the set  $\mathbb{Y}^-$ .
- Step 2. Design individual SISO controllers to compute the input for each CV constraint ( $u_i$ ) and for the CV setpoint controller ( $u_0$ ).
- Step 3. Use a minimum selector block to choose the largest allowed input  $\bar{u}$  that satisfies all the constraints in the set  $\mathbb{Y}^+$ , and use a maximum selector block to choose the smallest allowed input  $\underline{u}$  that satisfies all the constraints in the set  $\mathbb{Y}^-$ . The problem is feasible, that is, the set of constraints are not conflicting if  $\bar{u} > \underline{u}$  ([Theorem 1](#)).
- Step 4. When the problem is feasible, the optimal input is given by  $u = \text{mid}(\underline{u}, u_0, \bar{u})$  where  $u_0$  is the control input computed by the controller that controls the CV with a setpoint that can be given up ([Theorem 2](#)).
- Step 5. To handle infeasibility, use a max-min structure ([Fig. 4c](#)) if the constraints in  $\mathbb{Y}^-$  can be given up, or use a min-max structure ([Fig. 4b](#)) if the constraints in  $\mathbb{Y}^+$  can be given up ([Theorem 3](#)).

#### 4. Active constraint control using back-off

Due to imperfect control or measurement noise, sometimes it may be desirable to add a safety margin, known as *back-off*, where the setpoint is offset by a constant value from its limit. Back-off may also be used to simplify the control structure design since the same controller may be used in the different active constraint regions. However, there is an economic loss introduced by back-off, and quantifying this loss can help the designer in deciding whether tight control is required for some CV constraints.

Consider the steady-state optimization problem (1), which is now rewritten as

$$\min_{\mathbf{w}} J(\mathbf{w}) \text{ s.t. } \mathbf{g}_A(\mathbf{w}) + \boldsymbol{\varepsilon} = 0 \quad (13b)$$

where  $\mathbf{w} := [\mathbf{x}^T, \mathbf{u}^T]^T$  denotes the combined input and state variables, and  $\boldsymbol{\varepsilon} \geq 0$  is the back-off (safety margin) for the set of active constraints  $\mathbf{g}_A$ . Note that we only consider the active constraints and hence  $\boldsymbol{\varepsilon} \in \mathbb{R}^{n_a}$ . We have also eliminated  $\mathbf{d}$  for the sake of simplicity, since we are interested in quantifying the loss w.r.t the back-off  $\boldsymbol{\varepsilon}$  for a given disturbance. This can be seen as a parametric optimization problem, where we are interested in analyzing the effect of the back-off parameter  $\boldsymbol{\varepsilon}$  on the cost. The following theorem says that the loss is given by the value of the corresponding Lagrange multipliers,  $\lambda$ .

**Theorem 4** (Loss of back-off). Assume that the optimization problem (13) has an unique primal and dual solution  $\mathbf{w}^*(\boldsymbol{\varepsilon})$  and  $\lambda^*(\boldsymbol{\varepsilon})$  respectively. Then the steady-state loss due to a small non-zero back-off  $\boldsymbol{\varepsilon}$  is given by

$$\text{Loss} = J^*(0) - J^*(\boldsymbol{\varepsilon}) = -\lambda^*(0)^T \boldsymbol{\varepsilon} \quad (14)$$

**Proof.** See Appendix A  $\square$

The main implications of [Theorem 4](#) for control structure design are:

1. Determine which CVs need to be tightly controlled: If the Lagrange multiplier  $\lambda_i$  for a given constraint is large, then this constraint must be controlled tightly in order to minimize the losses.

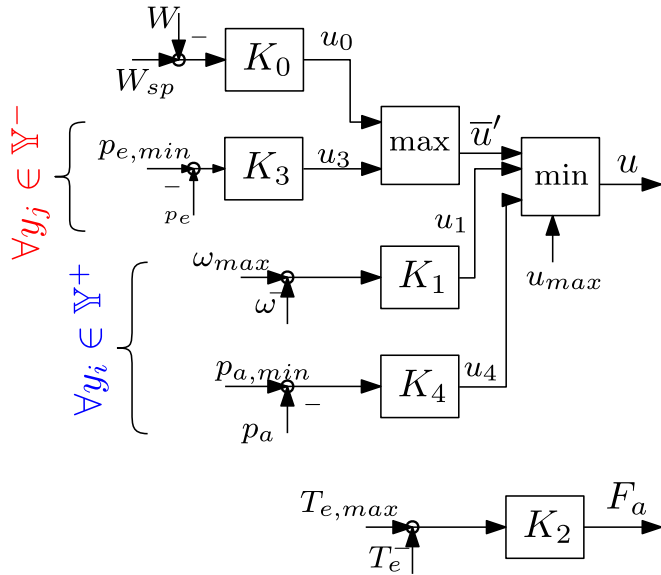


Fig. 5. Example 1: Proposed max-min control structure design for gas turbine control.

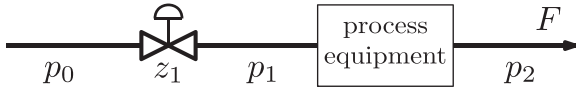


Fig. 6. Example 2: Flow through a pipe with one MV ( $u = z_1$ ).

2. Simplify control structure design: If the Lagrange multiplier  $\lambda_i$  for a given constraint is sufficiently small such that the loss is negligible/acceptable, then one can allow a large back-off, thus simplifying the control structure design (Govatsmark and Skogestad, 2005).

### 5. Illustrative examples

#### 5.1. Revisiting example 1 (gas turbine)

We now apply the systematic approach presented in the previous section to check for consistency and design a control structure for the motivating example introduced in Section 2.

Since the engine temperature  $y_2 = T_e$  is controlled to its limit of  $T_{e,max}$  using the air inflow rate  $F_a$ , we need to design control structures for the rest of the CVs using the fuel  $u$  as the MV. For this MV  $u$ , the constraints can be grouped into

$$Y^+ = \{\omega_{max}, p_{a,min}, u_{max}\}$$

$$Y^- = \{p_{e,min}\}$$

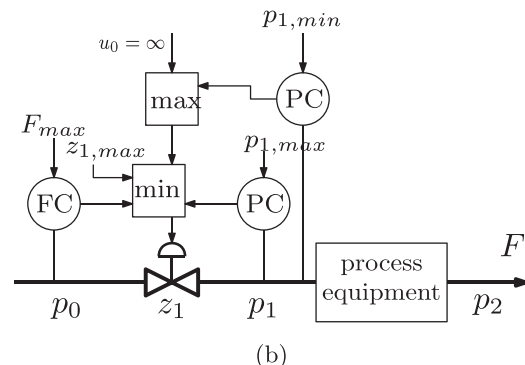
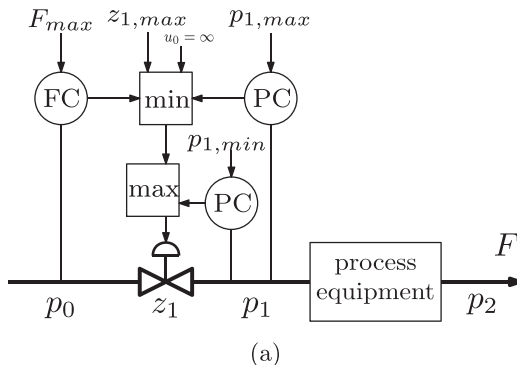


Fig. 7. Example 2: Two alternative control structures for constraint switching using selectors. (a) Min-max structure, see (9) (b) Max-min structure, see (10).

Since we have both set  $Y^+$  and  $Y^-$ , we do not have the special case where we can use a single selector block. The problem is feasible only if  $\underline{u} > \bar{u}$  (Theorem 1) where

$$\underline{u} = \min(u_1, u_4, u_{max})$$

$$\bar{u} = u_3$$

In the case of infeasibility, we will give up the constraint on  $Y^- = \{p_{e,min}\}$ . From Theorem 3, the resulting control structure is using a maximum followed by minimum (max-min) selector block as shown in Fig. 5.

This example demonstrates that the use of the proposed systematic procedure to design selector blocks is straightforward and leads to simple design.

#### 5.2. Example 2: Flow through a pipe

Consider a simple example of flow through a pipe with a valve placed upstream of some processing equipment as shown in Fig. 6. There is no accumulation in the processing equipment (i.e. inflow = outflow =  $F$ ), but there is a pressure drop across the equipment from  $p_1$  to  $p_2$ . This could be for example, a filter, a long pipe section, or some kind of a flow restriction or an orifice, the details of which are not important, since the models nor information about the equipment are not used in the control structure design. The valve  $z_1$  is a control valve which is assumed to be the only available degree of freedom. The objective is to maximize the flow rate  $F$  by manipulating the valve position  $u = z_1$ , subject to constraints on the flow rate  $F$ , downstream choke pressure  $p_1$  and valve opening  $z_1$ . The boundary pressures  $p_0$  and  $p_2$  are disturbances. The optimization problem is:

$$\max_{z_1} F$$

s.t.

$$F \leq F_{max} \tag{15}$$

$$p_1 \leq p_{1,max}$$

$$p_1 \geq p_{1,min}$$

$$z_1 \leq z_{1,max}$$

where  $F_{max} = 10$  kg/s,  $z_{1,max} = 1$ ,  $p_{1,max} = 2.5$  bar, and  $p_{1,min} = 1.5$  bar. Note that there are both max and min- constraints on  $p_1$ . Depending on the disturbances, one of these constraints may be optimally active at any given time, and the CV that needs to be controlled using  $z_1$  needs to be switched to remain optimal and feasible.

The constraints can be grouped into

$$Y^+ = \{F_{max}, p_{1,max}, z_{1,max}\}$$

$$Y^- = \{p_{1,min}\}$$

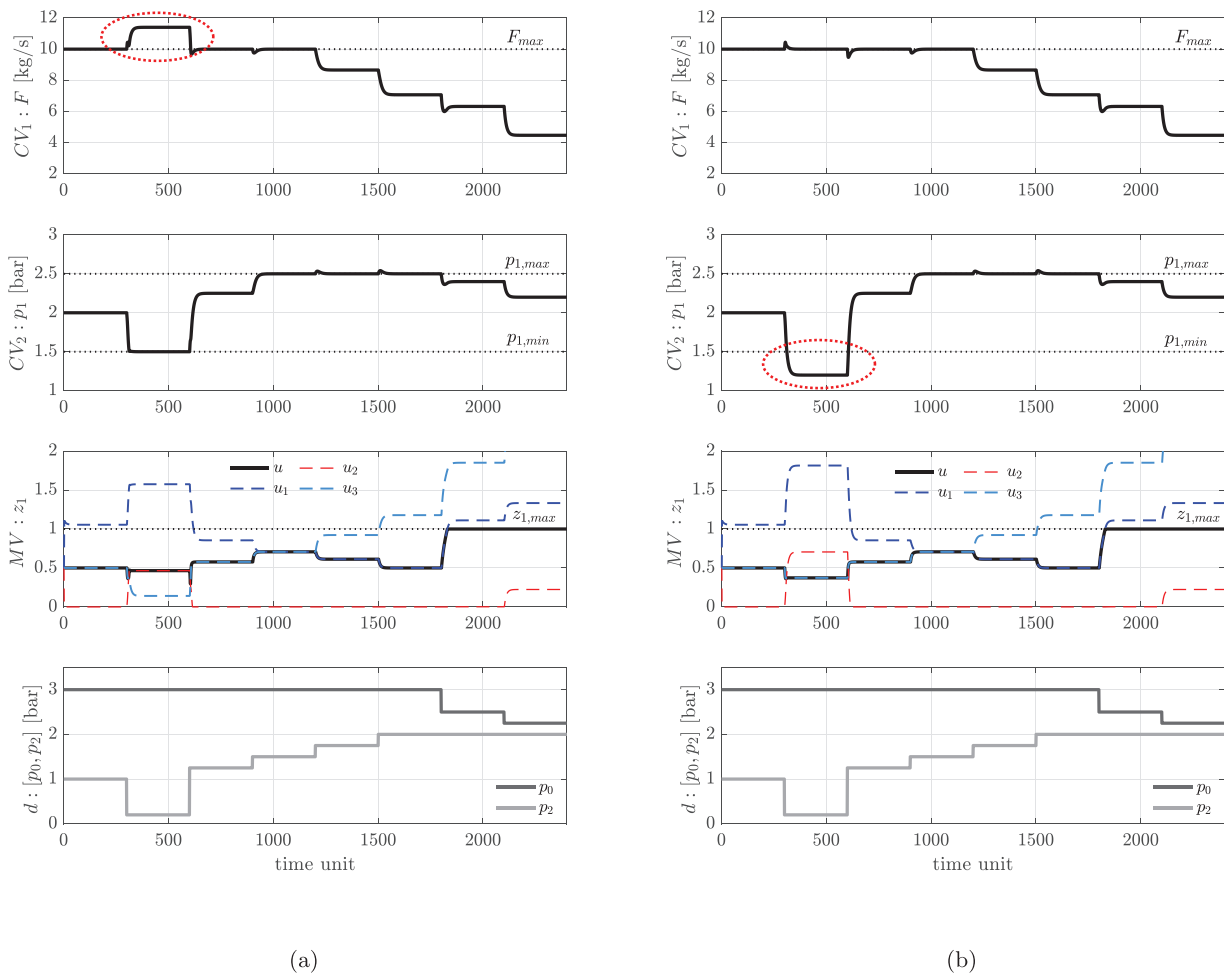


**Fig. 8.** Example 2: Simulation results (a) using the min-max control structure in Fig. 7a (b) using the max-min control structure in Fig. 7b. The control structures behave identical except between time  $t = 300$  s and  $t = 600$  s when operation is infeasible, and the structures violates different constraints (indicated by red dotted ellipses). (For interpretation of the references to colour in this figure legend, the reader is referred to the web version of this article.)

Since we have both sets  $\mathbb{Y}^+$  and  $\mathbb{Y}^-$ , we need at least two selector blocks, and we consider the max-min and min-max structures in Fig. 7. Note that since the objective is to maximize production, we have  $u_0 = \infty$  (for the imaginary unconstrained case). This value will not affect the operation, except that it will lead to maximizing  $u$ .

We use three SISO controllers to control the three CV constraints, namely,

1. Pressure controller that uses  $z_1$  to control  $y_1 = p_1$  to  $p_{1,max}$ . The output from this controller is  $u_1$ .
2. Pressure controller that uses  $z_1$  to control  $y_2 = p_1$  to  $p_{1,min}$ . The output from this controller is  $u_2$ .
3. Flow controller that uses  $z_1$  to control  $y_3 = F$  to  $F_{max}$ . The output from this controller is  $u_3$ .

In addition, we have that the manipulated variable is constrained. Therefore, the input to one of the blocks is

4.  $u_{max} = z_{1,max}$

At any given time the control action  $u = z_1$  computed by one of these four controllers is implemented on the plant. We have that for this example,

$$\bar{u} = \min(u_1, u_3, u_{max})$$

$$\underline{u} = u_2$$

**Table 2**

Example 2: Controller gains.

	FC	PC for $y_1 = p_{1,max}$	PC for $y_2 = p_{1,min}$
$K_p$	0.2314	$1.1091 \times 10^{-5}$	$1.1091 \times 10^{-5}$
$K_I$	0.0231	$1.1091 \times 10^{-6}$	$1.1091 \times 10^{-6}$
$K_{aw}$	0.1	0.1	0.1

The controllers have integral action, so an anti-windup scheme is required to avoid integral windup when the controller is not selected. We use the back-calculation scheme, which is discussed in Section 6.4. The controller tuning parameters are shown in Table 2.

For disturbances in the boundary pressures  $p_0$  and  $p_2$ , simulation results with the two structures in Fig. 7 are shown in Fig. 8a and Fig. 8b, respectively<sup>1</sup>. We see that the responses are good and the simulation results are identical, except in the time period between  $t = 300$  s and  $t = 600$  s, where operation with all constraints being satisfied is infeasible, since  $\underline{u} > \bar{u}$  which violates Theorem 1.

For the min-max structure in Fig. 7a, we violate the maximum flow limit  $F_{max}$  which belongs to  $\mathbb{Y}^+$  (marked by a red dotted ellipse in Fig. 8a).

<sup>1</sup> For the plant simulator, the model for the flow  $F$  is given by,  $F = c_{v1} z_1 \sqrt{(p_0 - p_1) / \rho}$  where  $c_{v1} = 2 \times 10^{-3} \text{ m}^2$ ,  $\rho = 1000 \text{ kg/m}^3$  and the processing equipment is modeled as a flow through a restriction with  $c_{v2} = 10^{-3} \text{ m}^2$ .

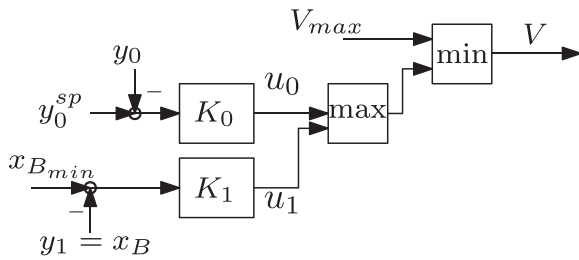


Fig. 9. Example 3: Feasible control structure to switch between the three active constraint regions R-I, R-II and R-III.

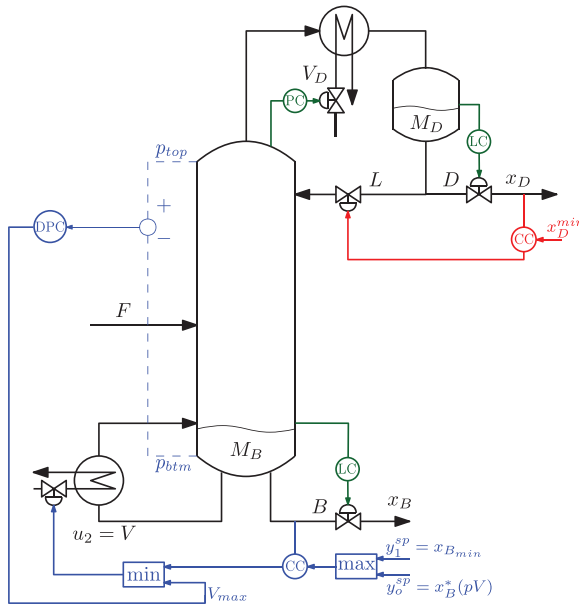


Fig. 10. Example 3: Proposed max-min control structure design for optimal operation of a two product distillation column over regions R-I, R-II, and R-III. Control loops that does not have an impact on the steady-state economics are shown in green. The the most valuable product that will always be active is shown in red. The control structure with the max and min-selectors to switch between R-I,R-II and R-III is shown in blue. (For interpretation of the references to colour in this figure legend, the reader is referred to the web version of this article.)

For the max-min structure in Fig. 7b, we instead violate the minimum pressure limit  $p_{1,min}$  which belongs to  $\mathbb{Y}^-$  (marked by a red dotted ellipse in Fig. 8b).

In order to say which structure is the best, this would depend on whether it is acceptable to violate the constraint on  $F_{max}$  or  $p_{1,min}$  (cf. Theorem 3). If its not possible to violate any of these constraints, then the safety system will need to be activated. Of course, it will be not activated immediately, because some back-off to the hard constraint has most likely been used.

### 5.3. Example 3: Distillation column

We consider a standard two-product distillation column, which is based on the ‘‘Column A’’ model used by Jacobsen and Skogestad (2011). The distillation column has 41 stages, including the re-boiler and the total condenser, with the feed entering at stage 21. The column splits a binary mixture with relative volatility of  $\alpha = 1.5$  into a top product  $D$  and a bottom product  $B$  as shown in Fig. 10. The model assumes constant relative volatility, constant

molar flows, no vapour holdup, linearized liquid dynamics and equilibrium on all stages<sup>2</sup>.

For a given feed rate of  $F$ , the distillation column has five dynamic degrees of freedom, namely, the reflux  $L$ , boilup  $V$ , overhead vapour  $V_D$ , distillate  $D$  and the bottom flow  $B$ . However, stable operation of the column requires control of the two levels  $M_B$  and  $M_D$  and the column pressure, which does not have any affect on the steady-state economics. The distillate  $D$ , bottom flow  $B$  and overhead vapour  $V_D$  are thus used in the regulatory layer to tightly control the levels  $M_D$ ,  $M_B$ , and the column pressure respectively as shown in Fig. 10 (in green). This leaves us with two steady-state degrees of freedom, namely, the reflux  $L$  and boilup  $V$  that can be used to optimize the process.

The objective is to minimize the operating costs and maximize revenue from the products. In addition, there are purity constraints on the top and bottom products, and constraints on the boilup  $V$ . The steady-state optimization problem is formulated as,

$$\begin{aligned} \min_{L,V} J &= p_F F + p_V V - p_D D - p_B B \\ \text{s.t.} \quad &x_D \geq x_{D,min} \text{ (always active)} \\ &x_B \geq x_{B,min} \\ &V \leq V_{max} \end{aligned} \tag{16}$$

where  $p_F$ ,  $p_V$ ,  $p_D$ , and  $p_B$  are the prices for the feed, energy, top product, and bottom product respectively. We assume that the energy price is a disturbance and varies between  $p_V \in [0.007, 0.02] \$/mol$ , whereas the other prices are constant at  $p_F = 1 \$/mol$ ,  $p_B = 1 \$/mol$  and  $p_D = 2 \$/mol$ .

The most valuable product constraint  $x_{D,min}$  will always be active at the optimum, because this avoids product giveaway, as explained by Jacobsen and Skogestad (2011). Thus we always have  $x_D = x_{D,min}$ . Therefore the relevant active constraint combinations are

- only  $x_D$  active (R-I)
- $x_D$  and  $y_c = x_B$  active (R-II)
- $x_D$  and  $u = V$  active (R-III)

Due to the pair-close rule, the reflux  $L$  is used to control  $x_D$  to its limit of  $x_{D,min} = 0.95$  as shown in Fig. 10 (in red).

This leaves one degree of freedom, namely the boilup  $u = V$ . For this MV, we may need to control the concentration  $x_B$  at its limit of  $x_{B,min} = 0.99$  (R-II), or control a self-optimizing variable  $y_0$  to a desired setpoint (R-I). In this example, we consider  $y_0 = x_B$  controlled to an economically optimal setpoint given as a function of the energy price  $x_{B,sp}(p_V)$  which is determined offline.

We use two SISO controllers to control the two CVs, namely,

1. Concentration controller that uses  $V$  to control  $y_1 = x_B$  to  $x_{B,min}$ . The output from this controller is  $u_1(x_B = x_{B,min})$ . (Active in R-II)
2. Concentration controller that uses  $V$  to control  $y_0 = x_B$  to  $x_{B,sp}$  (unconstrained case). The output from this controller is  $u_0(x_B = x_{B,sp})$ . (Active in R-I)

In addition, we have that the manipulated variable is constrained. Therefore, we also have

3.  $u_{max} = V_{max}$ . (Active in R-III)

Note that the limit  $V_{max}$  could be to avoid flooding in the column, and may, for example, be computed by a pressure drop (DP) controllers as shown in Fig. 10.

<sup>2</sup> Detailed model description and the MATLAB codes can be found in the attached supplementary information or in <http://folk.ntnu.no/skoge/distillation/>.



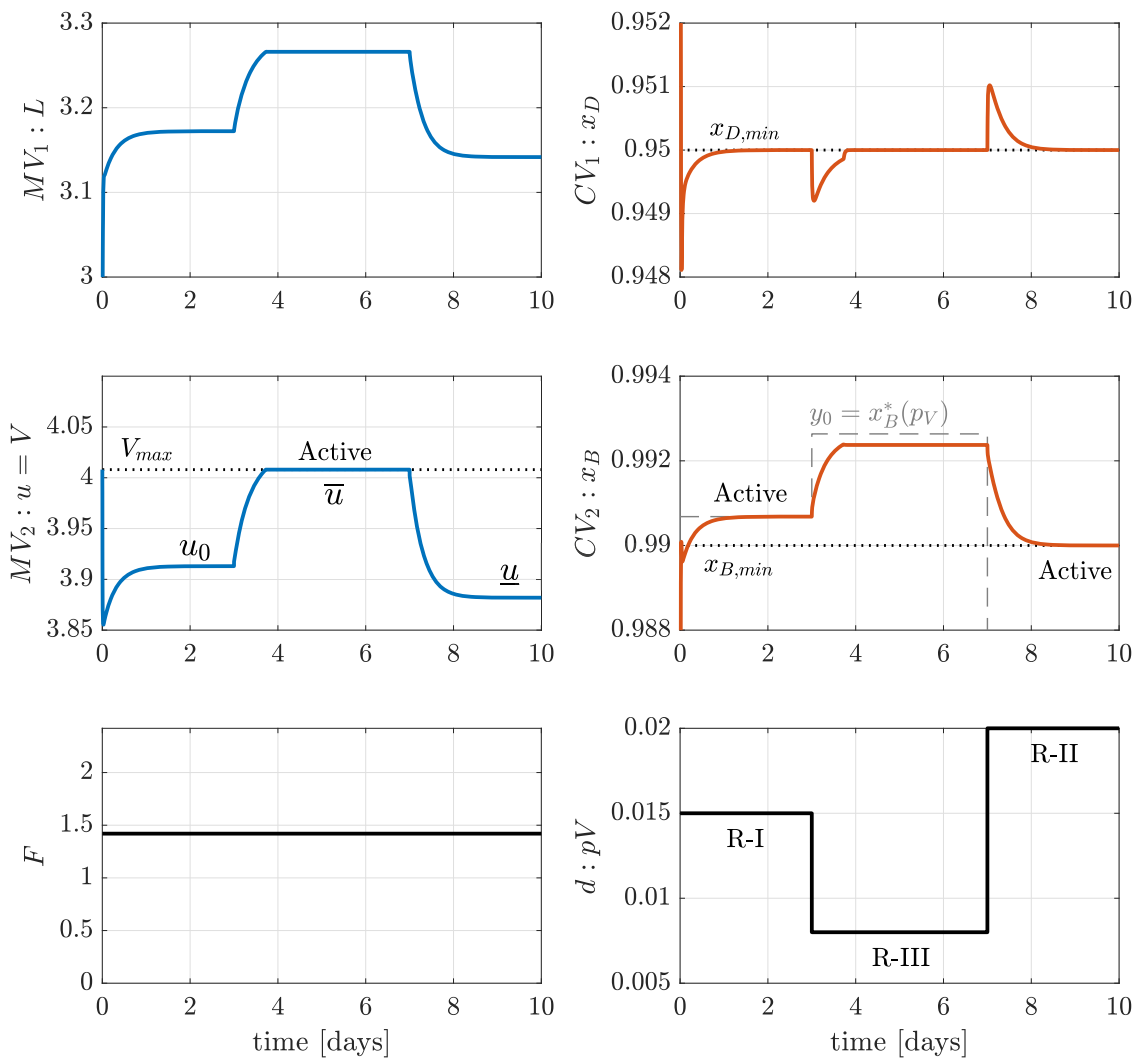


**Fig. 11.** Example 3: Closed loop simulation results for the distillation column with varying energy prices ( $d = p_V$ ). The control scheme in Fig. 10 achieves optimal steady-state operation in all the three constraint regions. The initial response is the start-up period because the column is not operated optimally at  $t = 0$ . (For interpretation of the references to colour in this figure legend, the reader is referred to the web version of this article.)

In this case,

$$\mathbb{Y}^+ = \{V_{max}\}$$

$$\mathbb{Y}^- = \{x_{B,min}\}$$

Optimal operation can be achieved using a mid-selector, or a combination of maximum and minimum selectors. Since we cannot give-up on the constraint  $V_{max} \in \mathbb{Y}^+$ , we choose to use a max-min selector as shown in Fig. 10 (Theorem 3). Furthermore, since the max-selector is used to switch between  $x_B$  being controlled to  $x_{B,min}$  and  $x_B$  being controlled to  $x_{B,sp}(p_V)$ , we can instead move the max-selector to the setpoint of the composition controller (CC), as shown in Fig. 10.

The simulation results for varying energy price  $p_V$  using the proposed control structure is shown in Fig. 11. It can be clearly seen that the proposed control structure is able to handle the active constraint switching as the disturbance changes. The concentration controller for  $x_B$  was implemented with anti-windup using input resetting to avoid integral windup. The detailed model and control structure design procedure for this example can be found in the supplementary information.

#### 5.4. Example 4: Williams-Otto reactor

The use of selector to switch between different active constraint regions is also tested on a benchmark Williams-Otto reactor example (Williams and Otto, 1960), which can be found in the attached supplementary information.

## 6. Discussion

Some switching logic blocks commonly used in practice can be seen as a special case of the CV-CV and CV-MV switching structures presented above. The developed framework is also applicable to such special cases. In this section, we first point out some of these special cases, and also discuss dynamic implementation aspects.

### 6.1. Mid-selector for zone control

Mid-selector block is often used in zone control (also known as range control), where the same output has both an upper and lower limit,  $y_{max}$  and  $y_{min}$ , respectively, and we have a desired value for the input  $u_0$  which may be varying. In this case,  $\mathbb{Y}^+ = \{y_{max}\}$  and  $\mathbb{Y}^- = \{y_{min}\}$ , and we have two different controllers to

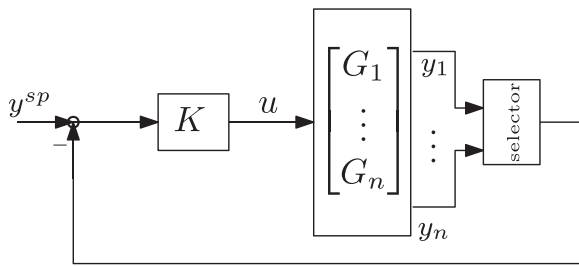


Fig. 12. Auctioneering as a special case of CV-CV switching, where the CVs  $y_1 \dots y_n$  all have the same units and same setpoint  $y^{sp}$ .

control  $y$  to  $y_{max}$ , and  $y$  to  $y_{min}$ , respectively. Since the limits are on the same output  $y$ , Theorem 1 is always satisfied. For example,  $y$  may be the temperature in a room, which we want to maintain between  $T_{min}$  and  $T_{max}$ , with a desired value for the input  $u_0$ . It is also possible to let  $u_0$  be the output of a third controller that controls  $y$  to a variable setpoint, which may be the optimal value for  $y$  when the constraints are not active.

### 6.2. Auctioneering

The proposed framework can also be used in *autioneering* control (Shinsky, 1996), which is a special case of CV-CV switching where we have similar CVs, i.e. the CVs have the same units and same setpoint. For example, we want to control the maximum temperature along a reactor or control the maximum opening for two valves. Then the selector may be on the output instead, i.e.  $y = \max(y_i)$  or  $y = \min(y_i)$ . In this case, we only need one controller, and a selector block chooses the lowest or highest measurement as feedback, as shown in Fig. 12. Another special case is when one needs to switch between a setpoint control and constraint control on the same variable. In this case, the selector may be used on the setpoint such that we only need one controller. This is also shown for the distillation column example in Fig. 10.

### 6.3. Input saturation

Typically in process control, the MV represents the actual physical manipulated variable. In this case, one does not even need the selector block for  $u_{max}$  or  $u_{min}$ , since the MV will physically saturate, e.g. max opening of a valve. However, when we use cascade control, the MV may be the setpoint to another controller. In this case, we need to include the constraint ( $u_{max}$  or  $u_{min}$ ) explicitly as shown in Fig. 4. This is sometimes referred to as clipping the controller output.

### 6.4. Dynamic implementation and anti wind-up

The theorems presented in Section 3 are based on steady-state analysis. Recall that  $u_i$  was defined as the value of the input  $u$  which at steady-state satisfies the constraint  $y_i = y_{i,lim}$ . However, the values for  $u_i$  computed by the controllers not selected are not equal to the correct values for  $u_i$  even at steady-state, but this is not a problem in practice.

When using selectors, only one of the control actions computed by a plurality of controllers is implemented on the plant at any given time. For the controllers that are not selected, the feedback loop is "broken" and the integral term may build up (known as *windup*), since the tracking error  $e_i = y_{i,sp} - y_i$  is non-zero<sup>3</sup>.

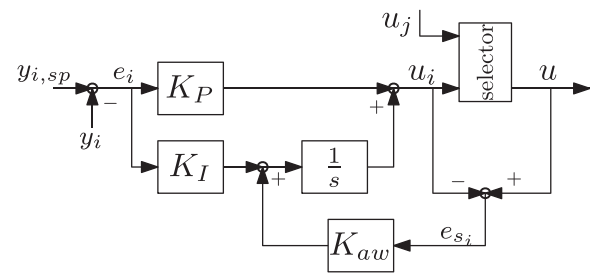


Fig. 13. PI controller with anti-windup.

This windup can be avoided using the back-calculation scheme where an additional feedback path is generated by using the difference between the output of the controller  $u_i$ , and the actual output  $u$  implemented on the plant  $u$  (Fertik and Ross, 1967), (Åström and Murray, 2010). This signal, denoted by  $e_{s_i} := u - u_i$  is fed back to the integrator with gain  $K_{aw_i}$  (as shown in Fig. 13) such that  $e_{s_i}$  goes towards zero when the controller is deselected. The PI controller with feedback anti-windup can be expressed as:

$$u_i(t) = K_P e_i(t) + \int_0^t (K_I e_i(\tau) + K_{aw_i} e_{s_i}(\tau)) d\tau \quad (17)$$

where  $e_i = y_{i,sp} - y_i$  is the tracking error,  $u_i$  is the control action computed by the  $i^{th}$  controller and  $u$  is the actual control action implemented on the plant,  $K_P$  and  $K_I$  are the proportional and integral gains respectively, and  $K_{aw_i}$  is the anti-windup feedback gain.

The integral action will drive the term in the integral to zero, so that at steady state we have

$$K_I e_i + K_{aw_i} e_{s_i} = 0 \quad (18)$$

In other words, at steady-state we have

$$u_i - u = \frac{K_I}{K_{aw_i}} e_i$$

If the controller is selected, then at steady-state  $e_i = 0$  and the feedback controller will generate the correct steady-state value for  $u_i$ . However, the steady-state value of  $u_i$  computed by the controller when  $u_i$  is not selected, depends on the parameter  $K_{aw_i}$ . So, it is clearly not the steady-state value that would give  $e_i = 0$ . Here,  $K_{aw_i}$  is a tuning parameter, and a large value of  $K_{aw_i}$  means that  $u_i(t)$  is close to  $u$ . A too large value of  $K_{aw_i}$  may activate  $u_i$  when its not necessary, for example, due to measurement noise for  $y_i$  or a change in  $y_i$  or  $y_{i,sp}$ , since changes in  $e_i = y_{i,sp} - y_i$  will affect  $u_i$  through the proportional term  $K_P e_i(t)$ .

A reasonable value for the anti-windup gain to avoid unnecessary activation for small change in  $y_i$  or  $y_{i,sp}$  is

$$K_{aw_i} = \frac{K_I}{K_P} \quad (19)$$

which means at steady-state we have

$$u_i - u = K_P e_i$$

In this case the proportional action  $K_P e_i$  will activate  $u_i$  only if  $e_i(t) = y_{i,sp} - y_i$  crosses zero, i.e. if  $y_i$  reaches its setpoint/constraint value.

To illustrate this, consider the flow example (Example 2 from Section 5.2). For  $p_0 = 1.75$  bar and  $p_2 = 3$  bar, the optimal operation occurs when the  $p_{1,max}$  constraint is active, with a flow rate of  $F = 8.66$  kg/s, as shown in Fig. 14. At time  $t = 300$  s, the maximum flow rate  $F_{max}$  is reduced from  $F_{max} = 10$  kg/s to  $F_{max} = 9$  kg/s. This, in principle, should not affect the operation, since  $F_{max} = 9$  kg/s will not be active. Indeed, with the chosen feedback gain of  $K_{aw} = 0.1$ , given by (19), we see from Fig. 14 (left hand side

<sup>3</sup> Note that for the active constraint controllers  $y_{i,sp} = y_{i,lim}$ .

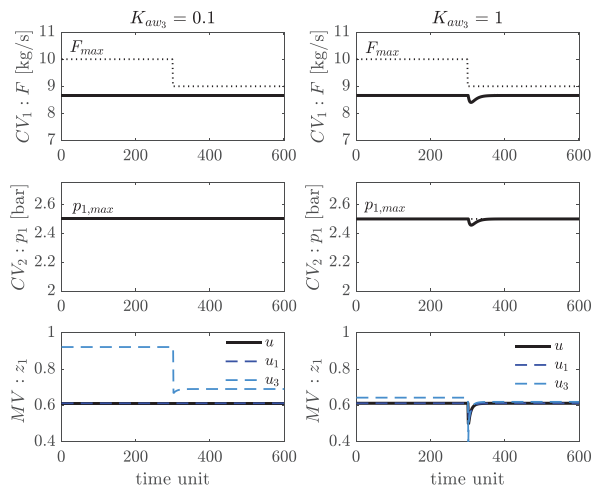


**Fig. 14.** Illustrative example showing that too large value of the anti-windup gain  $K_{aw}$  may lead to unnecessary switching of the controllers. The left hand side subplot shows the performance with the feedback gain chosen according to (19), and the right hand side subplot shows the same with  $K_{aw}$  10 times larger.

subplots) that the operation remains unchanged as one would expect. However, if we use the larger value of  $K_{aw} = 1$  we get unnecessary switching, with the flow controller becoming dynamically active before switching back to the pressure controller as shown in Fig. 14 (right hand side subplots).

### 6.5. Multiple inputs and conflicting constraints

This paper has considered the important case where all the constraints can be associated with a single input  $u$ . It is then possible to divide the constraints into the two sets  $\mathbb{Y}^+$  and  $\mathbb{Y}^-$ , which can be associated with min- and max-selectors, respectively.

In the case of multiple inputs, the proposed systematic design of selectors can be applied if each MV is paired with a set of constraints *a-priori*. For example, consider a process with  $n$  inputs  $v_i$ . If each MV  $v_i$  is paired with a set of constraints  $\mathbb{Y}_i$ , then this can be divided into two subsets  $\mathbb{Y}_i^+$  and  $\mathbb{Y}_i^-$  for all  $i = 1, \dots, n$ , which can each be associated with min- and max-selectors, respectively in a decentralized fashion. This was also seen in the gas turbine example in Fig. 5, where the air inlet flow was paired with  $T_{e,max}$ , and the fuel  $u$  was paired with the other remaining CVs.

In the case where two hard constraints from the set  $\mathbb{Y}_i$  cannot be satisfied at the same time, that is, we have infeasibility according to Theorem 1, then one needs to find some other input to take over one of the control tasks. Usually, this means that we need to give up some other control objective. For example, we may no longer be able to set the throughput freely, since we have reached a bottleneck for the process. In either case, this involves an MV-MV switching, which is not the scope of this paper. MV-MV switching may be achieved using split range control, input position control, and controllers with different setpoints. This has been studied in detail by Reyes-Lúa and Skogestad (2020, 2019); Reyes-Lúa et al. (2018). For example, in the distillation column example, when  $V_{max}$  is active, control of  $x_{B,min}$  is lost. If this is a hard constraint, then we would need to find another MV, such as the feed rate  $F$ , to control  $x_B$  to  $x_{B,min}$ . This is an MV-MV switching and this example is shown in detail by Reyes-Lúa and Skogestad (2020) using a combination of split range control and controllers with different setpoints.

A similar "override" distillation example with MV-MV switching from  $V$  to  $F$  using two controllers with different setpoints is given in (Kumar and Kaistha, 2019, Fig. 5) for a reactor-separator-recycle process. Note that since  $F$  is already used to control another

task (reactor level), the MV-MV switching from  $V$  to  $F$  has to be combined with a CV-CV switching (min-selector) for  $F$ . However, since also this task (reactor level) cannot be given up, this has to be combined with yet another override, MV-MV switch from  $F$  to  $FB$  (the throughput manipulator) which will reduce the feed  $FB$  to the reactor system.

In large multivariable systems with a lot of such CV-CV, CV-MV and MV-MV switchings, the control structure can quickly become complex, and perhaps one would then be better off with multivariable controllers such as model predictive control (MPC).

## 7. Conclusion

In this paper, we have presented a systematic procedure for designing selectors for CV-CV switching. Theorem 1 establishes the condition under which the constraints are feasible, and Theorem 2 shows that optimal operation can be achieved using minimum and maximum selector blocks in series. Theorem 3 tells us how the max-min and min-max selectors behave when used at conditions where satisfaction of the constraint is infeasible, and Theorem 3 tells us which structure to use based on the constraint priority list. The proposed systematic design framework does not require detailed process models, making it easily applicable and usable in industrial applications that are verifiable by design. The proposed framework was successfully demonstrated using several illustrative examples.

### Declaration of Competing Interest

The authors declare that they have no known competing financial interests or personal relationships that could have appeared to influence the work reported in this paper.

### Appendix A. Proof of Theorem 4

The Lagrangian function of (13) is given as

$$\mathcal{L}(\mathbf{w}, \boldsymbol{\varepsilon}, \boldsymbol{\lambda}) = J(\mathbf{w}) + \boldsymbol{\lambda}^\top (\mathbf{g}_A(\mathbf{w}) + \boldsymbol{\varepsilon}) \quad (\text{A.1})$$

The necessary conditions of optimality

$$\frac{\partial \mathcal{L}}{\partial \mathbf{w}} = \frac{\partial J}{\partial \mathbf{w}} + \boldsymbol{\lambda}^\top \frac{\partial \mathbf{g}_A}{\partial \mathbf{w}} = \mathbf{0} \mathbf{g}_A + \boldsymbol{\varepsilon} = \mathbf{0} \quad (\text{A.2b})$$

determines the optimal primal and dual variables  $\mathbf{w}^*(\boldsymbol{\varepsilon})$  and  $\boldsymbol{\lambda}^*(\boldsymbol{\varepsilon})$  respectively, as a function of the back-off parameter  $\boldsymbol{\varepsilon}$ , assuming there exists a unique solution for each  $\boldsymbol{\varepsilon}$ .

Since  $\mathcal{L}$  and  $\mathbf{g}$  depends on  $\boldsymbol{\varepsilon}$  through  $\mathbf{w}$ ,  $\boldsymbol{\lambda}$  and  $\boldsymbol{\varepsilon}$ , differentiating (A.2) gives

$$\frac{\partial^2 \mathcal{L}}{\partial \mathbf{w}^2} \frac{\partial \mathbf{w}^\top}{\partial \boldsymbol{\varepsilon}} + \frac{\partial^2 \mathcal{L}}{\partial \mathbf{w} \partial \boldsymbol{\varepsilon}} + \frac{\partial \mathbf{g}_A^\top}{\partial \mathbf{w}} \frac{\partial \boldsymbol{\lambda}}{\partial \boldsymbol{\varepsilon}} = \mathbf{0} \frac{\partial \mathbf{g}_A}{\partial \mathbf{w}} \frac{\partial \mathbf{w}^\top}{\partial \boldsymbol{\varepsilon}} + \mathbf{1} = \mathbf{0} \quad (\text{A.3b})$$

Let the optimal value function be denoted as  $J^*(\boldsymbol{\varepsilon}) = J(\mathbf{w}^*(\boldsymbol{\varepsilon}))$ , and the sensitivity of the optimal value function w.r.t  $\boldsymbol{\varepsilon}$  can be expressed as

$$\frac{\partial J^*(\boldsymbol{\varepsilon})}{\partial \boldsymbol{\varepsilon}} = \frac{\partial J}{\partial \mathbf{w}} \frac{\partial \mathbf{w}^\top}{\partial \boldsymbol{\varepsilon}} \quad (\text{A.4})$$

From (A.2a) and (A.3b), this can be rewritten as,

$$\frac{\partial J^*}{\partial \boldsymbol{\varepsilon}} = -\boldsymbol{\lambda}^*(\boldsymbol{\varepsilon})^\top \frac{\partial \mathbf{g}_A}{\partial \mathbf{w}} \frac{\partial \mathbf{w}^\top}{\partial \boldsymbol{\varepsilon}} = \boldsymbol{\lambda}^*(\boldsymbol{\varepsilon})^\top \quad (\text{A.5})$$

The loss due to a back-off of  $\boldsymbol{\varepsilon} > \mathbf{0}$  is the where  $\boldsymbol{\lambda}^*(\mathbf{0})$  is the Lagrange multiplier for the active constraints without back-off. Therefore it can be seen that the loss scales linearly with the back-off.

## Supplementary material

Supplementary material associated with this article can be found, in the online version, at doi:[10.1016/j.compchemeng.2020.107106](https://doi.org/10.1016/j.compchemeng.2020.107106).

## CRediT authorship contribution statement

**Dinesh Krishnamoorthy:** Conceptualization, Methodology, Software, Validation, Formal analysis, Writing - original draft, Writing - review & editing. **Sigurd Skogestad:** Conceptualization, Methodology, Formal analysis, Writing - review & editing.

## References

- Ariyur, K.B., Krstic, M., 2003. Real-time optimization by extremum-seeking control. John Wiley & Sons.
- Åström, K.J., 1987. Advanced control methods: Survey and assessment of possibilities. K.J.
- Åström, K.J., Murray, R.M., 2010. Feedback systems: An introduction for scientists and engineers. Princeton university press.
- Chachuat, B., Srinivasan, B., Bonvin, D., 2009. Adaptation strategies for real-time optimization. *Computers & Chemical Engineering* 33 (10), 1557–1567.
- Engell, S., 2007. Feedback control for optimal process operation. *J. Process Control* 17 (3), 203–219.
- Fertik, H.A., Ross, C.W., 1967. Direct digital control algorithm with anti-windup feature. *ISA Trans.* 6 (4), 317.
- Foss, A.M., 1981. Criterion to assess stability of a 'lowest wins' control strategy.
- François, G., Srinivasan, B., Bonvin, D., 2005. Use of measurements for enforcing the necessary conditions of optimality in the presence of constraints and uncertainty. *J. Process Control* 15 (6), 701–712.
- Glattfelder, A., Schaufelberger, W., 1983. Stability analysis of single loop control systems with saturation and antireset-windup circuits. *IEEE Trans. Automat. Contr.* 28 (12), 1074–1081.
- Glattfelder, A.H., Schaufelberger, W., 2012. Control systems with input and output constraints. Springer Science & Business Media.
- Govatsmark, M.S., Skogestad, S., 2005. Selection of controlled variables and robust setpoints. *Industrial & engineering chemistry research* 44 (7), 2207–2217.
- Gros, S., Srinivasan, B., Bonvin, D., 2009. Optimizing control based on output feedback. *Computers & Chemical Engineering* 33 (1), 191–198.
- Imani, A., Montazeri-Gh, M., 2020. Stability analysis of override logic system containing state feedback regulators and its application to gas turbine engines. *European Journal of Control* 52, 97–107.
- Jacobsen, M.G., Skogestad, S., 2011. Active constraint regions for optimal operation of chemical processes. *Industrial & Engineering Chemistry Research* 50 (19), 11226–11236.
- Jagtap, R., Kaistha, N., Luyben, W.L., 2013. External reset feedback for constrained economic process operation. *Industrial & Engineering Chemistry Research* 52 (28), 9654–9664.
- Jäschke, J., Cao, Y., Kariwala, V., 2017. Self-optimizing control—a survey. *Annu. Rev. Control.*
- Krishnamoorthy, D., Skogestad, S., 2019. Online process optimization with active constraint set changes using simple control structures. *Industrial & Engineering Chemistry Research*.
- Krishnamoorthy, D., Skogestad, S., 2020. Linear gradient combination as self-optimizing variables. *Computer Aided Chemical Engineering* In-Press.
- Kumar, V., Kaistha, N., 2014. Hill-climbing for plantwide control to economic optimum. *Industrial & Engineering Chemistry Research* 53 (42), 16465–16475.
- Kumar, V., Kaistha, N., 2019. Real-Time optimization of a reactor–Separator–Recycle process II: dynamic evaluation. *Industrial & Engineering Chemistry Research* 58 (5), 1966–1977.
- Liptak, B.G., 2003. Instrument Engineers' handbook, volume one: Process measurement and analysis. CRC press.
- Marlin, T.E., 2000. Process control, designing processes and control systems for dynamic performance, 2nd McGraw Hill, New York.
- Morari, M., Arkun, Y., Stephanopoulos, G., 1980. Studies in the synthesis of control structures for chemical processes: part i: formulation of the problem. process decomposition and the classification of the control tasks. analysis of the optimizing control structures. *AIChE J.* 26 (2), 220–232.
- Reyes-Lúa, A., Skogestad, S., 2019. Multiple-input single-output control for extending the steady-state operating range of controllers with different setpoints. *Processes* 7 (12), 941.
- Reyes-Lúa, A., Skogestad, S., 2020. Systematic design of active constraint switching using classical advanced control structures. *Industrial & Engineering Chemistry Research* 59, 2229–2241.
- Reyes-Lúa, A., Zoticá, C., Skogestad, S., 2018. Optimal operation with changing active constraint regions using classical advanced control. *IFAC-PapersOnLine* 51 (18), 440–445.
- Seborg, D.E., Mellichamp, D.A., Edgar, T.F., Doyle III, F.J., 2010. Process dynamics and control. John Wiley & Sons.
- Shinskey, F.G., 1996. Process control systems: Application, design, and tuning, 4. McGraw-Hill New York.
- Skogestad, S., 2000. Plantwide control: the search for the self-optimizing control structure. *J. Process Control* 10 (5), 487–507.
- Smith, C.A., Corripio, A.B., 2006. Principles and practice of automatic process control, 3 Wiley New York.
- Srinivasan, B., Bonvin, D., 2019. 110th anniversary: a feature-based analysis of static real-time optimization schemes. *Industrial & Engineering Chemistry Research* 58 (31), 14227–14238.
- Wade, H.L., 2004. Basic and advanced regulatory control: System design and application. ISA.
- Williams, T.J., Otto, R.E., 1960. A generalized chemical processing model for the investigation of computer control. *Transactions of the American Institute of Electrical Engineers, Part I: Communication and Electronics* 79 (5), 458–473.